



## Modeling isotherm and mechanism adsorption of heavy metals from water using brut keratin powder prepared from Algerian sheep horns

Fatiha Sidiali<sup>a</sup>, Rafika Souag<sup>a,\*</sup>, Nesrinne Seddiki<sup>b</sup>

<sup>a</sup>Research Unit, Materials, Processes and Environment (URMPE), University of Boumerdes, Boumerdes 35000, Algeria, Tel.: (213) 661751789; email: r.souag@univ-boumerdes.dz (R. Souag), Tel.: (+213) 7900017965; email: bouzidwassimohamed@gmail.com (F. Sidiali)

<sup>b</sup>Laboratory of Polymers Treatment and Forming, Université of Boumerdes, Boumerdes 35000, Algérie, Tel.: (+213) 782647632; email: n.seddiki@univ-boumerdes.dz

Received 28 March 2023; Accepted 22 August 2023

### ABSTRACT

The batch removal of  $Pb^{2+}$ ,  $Cd^{2+}$ , and  $Zn^{2+}$  ions from aqueous solution using brut keratin powder prepared from Algerian sheep horns (BKASH) were investigated. The BKASH before and after biosorbent was characterized using Fourier-transform infrared spectroscopy and scanning electron microscopy. The study investigated the effects of pH, contact time, biosorbent dose, initial ion concentration, and temperature on the removal of these heavy metal ions. The results indicated that the optimal conditions for adsorption were an initial concentration of 20 mg/L for 30 min. The monolayer adsorption capacities of  $Pb^{2+}$ ,  $Cd^{2+}$ , and  $Zn^{2+}$  were found to be 33.33, 23.81, and 25 mg/g, respectively, at 298 K. The maximum efficiency of  $Pb^{2+}$ ,  $Cd^{2+}$ , and  $Zn^{2+}$  adsorption was obtained at pH values of 4.5, 6, and 4.5, respectively, which is higher than the adsorbent's  $pH_{ZPC}$  of 4.3. The experimental data was fit with Langmuir, Freundlich, Temkin and Elovich isotherm models, and the best coefficient of determination was deduced by Langmuir isotherm. Three models were used to evaluate the kinetics of the process, including pseudo-first-order, pseudo-second-order kinetic models and intraparticle diffusion. The pseudo-second-order model was found to have the best correlation for the adsorption of  $Pb^{2+}$ ,  $Cd^{2+}$ , and  $Zn^{2+}$  on BKASH. Thermodynamic parameters were calculated and discussed. The negative  $\Delta G^\circ$  and positive  $\Delta H^\circ$  values indicated that the overall adsorption was spontaneous and endothermic. Overall, the study demonstrated that BKASH biosorbent has satisfactory biosorption capacity and can be considered an effective biosorbent for water treatment with a low concentration of heavy metal ions.

**Keywords:** Algerian sheep horns; Keratin powder; Adsorption; Isotherm; Equilibrium; Kinetics

### 1. Introduction

The increasing discharge of industrial wastewater from metallurgy, electroplating, petroleum, and other sources is negatively affecting water quality. The release of undesirable pollutants, such as heavy metals [1,2], significantly impacts water quality, which is a significant issue because high concentrations of heavy metals are toxic to aquatic ecosystems, living organisms, plants, and humans. Typical heavy metal

contaminants include chromium, lead, cadmium, zinc, copper, mercury, etc., which are non-biodegradable and can cause brain and bone damage, damage to the nervous system, neurological disorders, and even cancer [3,4]. The World Health Organization (WHO) recommended maximum levels of lead, zinc, and cadmium in water as 0.01, 5, and 0.005, respectively, in 1996 [5]. Therefore, an efficient and environmentally friendly method is required to purify contaminated water.

\* Corresponding author.

Various techniques are used to remove heavy metal ions from industrial effluents, such as chemical precipitation [6,7], reverse osmosis [8], nanofiltration, and ultrafiltration [9,10], ion-exchange [11], and the membrane process [12]. Among these methods, the adsorption technique is the most straightforward, cheapest, and fastest for heavy metal removal and is applicable for lower concentration levels. In adsorption, molecules of liquid are bound by the solid surface [13].

Recently, low-cost adsorbents developed from natural materials or certain waste materials from agricultural or industrial activities have gained greater attention due to their many apparent advantages, such as easy availability, comparable efficiency, resource generation, pollution reduction, and the use of several low-cost biomass materials [14]. Accordingly, various biogenic materials, including chitosan derivatives [15], agricultural waste materials [16], chicken feathers, cork waste [17–19], etc., have shown excellent sorption capacities for toxic metal ions in solutions.

Keratinous materials possess good biosorption properties attributed to their large metal-binding functional groups, such as carbonyl, carboxyl, hydroxyl, sulfur, amido, and amino groups. These materials exhibit excellent hydrophilicity and adsorption abilities, making them useful in treating heavy metal pollution. Keratinous materials have garnered increasing attention from researchers in recent years due to their abundance in wool, feathers, hair, animal claws, and horns [20–23]. Examples of the use of keratinous materials for heavy metal removal from aqueous solutions have been reported in previous research [17,18,24,25]. This material offers high adsorption capacity for heavy metal ions from water.

In the current study, brut keratin powder prepared from Algerian sheep horns (BKASH) was used to remove  $Pb^{2+}$ ,  $Zn^{2+}$ , and  $Cd^{2+}$  from aqueous solution. The study will analyze the influence of operating conditions, such as solution pH, biosorbent dosage, and contact time, on the sorption process. Additionally, it will calculate the adsorption capacity and metal removal efficiency, and evaluate kinetic models, equilibrium isotherm models, and thermodynamic parameters related to the adsorption process. Finally, the study will report on the mechanism of  $Cd^{2+}$ ,  $Zn^{2+}$ , and  $Pb^{2+}$  ion adsorption on BKASH.

## 2. Experimental set-up

### 2.1. Preparation of BKASH and characterization

The process of preparing the adsorbent involved collecting Algerian sheep's horns from butchers in the Boumerdes region. The horns were thoroughly cleaned using detergent to remove any residual soft tissue, followed by washing with tap and distilled water. They were then left to dry under sunlight for 2 d, and afterward, oven-dried at 353 K for 2 h to reduce their water content. The dried horns were cut into small pieces, ground, and sieved to achieve a uniform particle size. The adsorbent was not subjected to any other physical or chemical treatments during the preparation stage.

The functional groups of the biosorbent were analyzed using Fourier-transform infrared spectroscopy (FTIR) before and after adsorption. The surface morphology and

structure of BKASH were determined using scanning electron microscopy (SEM) equipped with an ESEM-FEG EDX probe. The adsorbent's zero-point charge was determined using the solid addition method in batch mode.  $NaNO_3$  solution (0.1 M) was transferred into a series of 100 mL conical flasks, and the initial pH values were adjusted between 2 to 13. After adding 0.1 g of adsorbent to each flask and shaking for 30 min, the flasks were kept at room temperature for 24 h to reach equilibrium. The pH values were measured using a digital pH meter before and after agitation.

### 2.2. Material and research equipment

The adsorbent used in this study was BKASH, and all chemicals used were of analytical-grade quality. A stock solution of ions (1,000 mg/L) was prepared by dissolving a suitable amount of the corresponding nitrate salt in deionized water. Working solutions were prepared by diluting the stock solution. Nitric acid and sodium hydroxide solutions were used to adjust the pH. The equipment used in this study included a mortar and pestle, sieve, analytical balance, spatula, pipette, vacuum pump, Duran Buchner Erlenmeyer flask and funnel, stopwatch, atomic absorption spectrophotometry (AAS) instrument (PerkinElmer, MAS 50, Mercury Analyzer), and some commonly used glassware. Data processing was carried out using OriginPro 8.5.0 SR1.

### 2.3. Batch adsorption studies

The effects of the experimental parameters, such as the initial concentration 20–100 mg/L, pH 1–6, adsorbent dose 0.02–1 g and temperature 298–313 K on the adsorptive removal of  $Pb^{2+}$ ,  $Cd^{2+}$  and  $Zn^{2+}$  ions are studied in batch mode for a specific period of contact time 0–60 min. For the batch experiments, 0.05 g of BKASH adsorbent was mixed with 20 mL of initial metal solution in a 100 mL glass bottle on a shaker with a stirring speed of 300 rpm.

After that, the suspensions were filtered each time using filter paper, and the metal concentrations remaining in the supernatant were analyzed by AAS.

All adsorption experiments were carried out at room temperature (298 K).

The amount of  $Pb^{2+}$ ,  $Cd^{2+}$ , and  $Zn^{2+}$  ions adsorbed on BKASH (mg/g) is calculated by using the following Eq. (1):

$$q_t = \frac{(C_0 - C_t) \cdot V}{m} \quad (1)$$

where  $C_0$  and  $C_t$  are the initial concentration and the concentration of  $Cd^{2+}$ ,  $Zn^{2+}$  and  $Pb^{2+}$  ions at any time (mg/L), respectively,  $V$  is the volume of heavy metal solutions (L), and  $m$  is the mass of BKASH biosorbent (g).

The removal efficiency  $R(\%)$  is evaluated using the following Eq. (2):

$$R\% = \frac{C_0 - C_e}{C_0} \times 100 \quad (2)$$

#### 2.3.1. Chi-square and the residual errors

Due to the inherent bias resulting from the linearization of the isotherm and kinetic model, the non-linear

regression (root mean square error, RMSE) evaluated in Eq. (3) is used as a criterion for the quality of fitting.

$$\text{RMSE} = \sqrt{\frac{1}{N-2} \sum_{i=1}^N (q_{e,\text{exp}} - q_{e,\text{cal}})^2} \quad (3)$$

where  $q_{e,\text{exp}}$  (mg/g) is the experimental value of uptake,  $q_{e,\text{cal}}$  is the calculated value of uptake using a model (mg/g), and  $N$  is the number of observations in the experiment (the number of data points).

The chi-square statistic is given as:

$$\chi^2 = \sum_{i=1}^N \frac{(q_{e,\text{exp}} - q_{e,\text{cal}})^2}{q_{e,\text{cal}}} \quad (4)$$

If the data from the model are similar to the experimental ones,  $\chi^2$  is small; by contrast, if they are different,  $\chi^2$  becomes large. The smaller the RMSE and  $\chi^2$  values, the better the curve fitting [26].

#### 2.4. Kinetics models and isotherm models

The kinetic study is important for the adsorption process because it describes the uptake rate of the adsorbate and controls the residual time of the whole process.

The pseudo-first-order and pseudo-second-order kinetics models were used to investigate the adsorption kinetics [27]. The first-order kinetic model can be used at the initial period of the first reaction step, and the second-order kinetic model is suitable to describe the whole adsorption process involving a chemical reaction.

The pseudo-first-order equation is given by the following Eq. (5):

$$q_t = q_e (1 - e^{-K_1 t}) \quad (5)$$

while the pseudo-second-order model is given by:

$$q_t = \frac{q_e^2 K_2 t}{1 + q_e K_2 t} \quad (6)$$

where  $q_t$  (mg/g): is the adsorption capacity of the keratin powder at a given time  $t$ ;  $q_e$  (mg/g): is the equilibrium adsorption capacity of the keratin powder;  $K_1$  ( $\text{min}^{-1}$ ): the first-order rate constant,  $K_2$  (mg/g·min): the second-order rate constant.

The adsorption isotherms measure the adsorbate distribution between liquid and solid phases at a constant temperature. The adsorption capacity depends on the adsorbent's affinity for the solute. The isotherm models help understand adsorption mechanisms and affinities. In this study, four isotherm models (Langmuir [28], Freundlich [29], Temkin and Elovich [30,31]) were used to discuss the  $\text{Pb}^{2+}$ ,  $\text{Cd}^{2+}$  and  $\text{Zn}^{2+}$  adsorption on BKASH.

### 3. Results and discussion

#### 3.1. Properties and characterizations

The physical and chemical characteristics of the powder prepared from the Algerian sheep horns are presented in Table 1.

The chemical characteristics of keratin horn powder indicate that carbon is the most abundant element. The high nitrogen content (15.16%) is due to keratin's presence. The adsorbent contained a significant amount of sulfur (2.76%), and the keratin powder is high in the sulfur-containing amino acid cysteine [32]. The other physical properties like bulk density, total porous volume, pH of BKASH are given in Table 1, which may affect the adsorption capacity.

$\text{pH}_{\text{ZPC}}$  is the pH at which adsorbents have a net zero surface charge. Fig. 1 shows the plot between  $\text{pH}_{\text{initial}}$  and  $\text{pH}_{\text{final}}$  for determining  $\text{pH}_{\text{ZPC}}$ . The results indicated that the  $\text{pH}_{\text{ZPC}}$  for BKASH was 4.3. The BKASH becomes more positively charged when pH is less than  $\text{pH}_{\text{ZPC}}$  and more negatively charged when pH is above  $\text{pH}_{\text{ZPC}}$ .

The FTIR spectra of BKASH before and after adsorption of  $\text{Pb}^{2+}$  are shown in Fig. 2. Generally, the absorption spectra of BKASH before and after the adsorption of heavy metal ions were similar. The presence of various functional groups such as carbonyl, carboxyl, and amide groups contributed to the appearance of several peaks in the infrared spectrum. In the range 3,000 at 3,800  $\text{cm}^{-1}$  from OH stretching, this peak C,O group connected to the amide group gives absorption peak at 1,670–1,700  $\text{cm}^{-1}$  in BKASH. Amide II at (1,400–1,500  $\text{cm}^{-1}$ ) showed the absorption of C–N stretching and N–H bending vibrations. The absorption area of amide III (1,220–1,300  $\text{cm}^{-1}$ ) indicated the absorption of N–H bending, C–N stretching on O=C–N bonds. S–S bonds

Table 1  
Characteristics of BKASH adsorbent

Physical characteristics	Chemical characteristics%
Moisture content, %	4.4 Nitrogen 15.16
Water content, %	4.2 Sulfur 2.76
Apparent density, g/mL	0.28 Hydrogen 6.27
Real density, g/mL	0.4 Oxygen 31.49
Total porous volume, $\text{m}^3/\text{g}$	1.01 Carbon 44.32
pH at 25°C	4.6

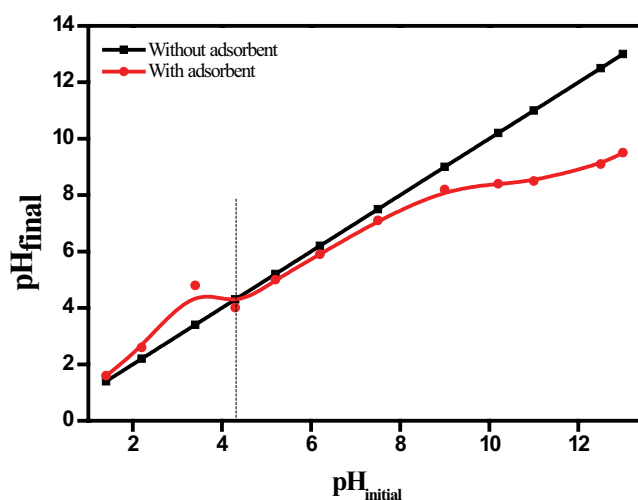


Fig. 1. Determination of  $\text{pH}_{\text{ZPC}}$ .

were confirmed with bands at  $1,054\text{ cm}^{-1}$  in BKASH, also the absorption band related to the C–S bond was observed at  $611\text{ cm}^{-1}$ . These results confirmed the protein nature of the adsorbent.

However, slight differences and redshifts of the emission spectra were observed before and after the biosorption process, which were likely due to the presence of heavy metal ions on the horn keratin surface. The scissor vibration of  $-\text{NH}_2$ , amide II, at  $1,445\text{ cm}^{-1}$  shifted to  $1,451\text{ cm}^{-1}$ , indicating the combination between  $\text{Pb}^{2+}$  and  $-\text{NH}_2$ . The C=O stretching vibration at  $1,637\text{ cm}^{-1}$ , related to  $-\text{CONH}-$ , namely the amide I belt, shifted to  $1,632\text{ cm}^{-1}$  after the biosorption process, indicating the coordination of  $\text{Pb}^{2+}$  and  $-\text{CONH}-$ . The peak located at  $1,054\text{ cm}^{-1}$  in BKASH before sorption shifted to  $1,065\text{ cm}^{-1}$  for BKASH after sorption of  $\text{Pb}^{2+}$ , suggesting the involvement of the carboxyl group of horn keratin in the sorption of metal ions. Moreover, Fig. 2 shows an increased intensity of the amide I and amide II bands after adsorption, indicating the hydrolysis of the amide bond into amino and carboxyl groups. The peak at  $612\text{ cm}^{-1}$ , assigned to C–S bond stretching and S–S bond stretching, shifted to  $624\text{ cm}^{-1}$  for BKASH after sorption of lead ions. Therefore, infrared analysis revealed the formation of complexes between metal ions and BKASH, which involved various functional groups responsible for binding the ions from the aqueous solution onto the surface of the adsorbent [33–36].

Images of BKASH through scanning electron micrographs before and after the adsorption of  $\text{Pb}^{2+}$  are depicted in Fig. 3a and b. The morphology of BKASH shown in Fig. 3a exhibits a porous structure. Furthermore, a significant number of wide pores were observed in the outer region of the material. This porous structure is highly advantageous for the purpose of adsorbing pollution. After the adsorption of  $\text{Pb}^{2+}$  ions, the surface morphology underwent a significant change (Fig. 3b). It is evident from this figure that a layer formed due to  $\text{Pb}^{2+}$  adsorption on the surface and that some  $\text{Pb}^{2+}$  ions have occupied the pores of BKASH.

### 3.2. Optimization study of operating conditions

#### 3.2.1. Effect of initial pH on uptake of $\text{Cd}^{2+}$ , $\text{Zn}^{2+}$ and $\text{Pb}^{2+}$

The adsorption process is greatly influenced by the pH of ion solutions, and it plays a crucial role in determining the uptake capacity of biosorbents. The impact of this parameter on BKASH's ability to adsorb  $\text{Cd}^{2+}$ ,  $\text{Zn}^{2+}$ , and  $\text{Pb}^{2+}$  ions at  $298\text{ K}$  is demonstrated in Fig. 4.

The results indicate that the adsorption capacity of  $\text{Mn}^+$  increases as the pH increases from 2 to 7, reaching its peak values of 7.98, 7.488, and  $6.51\text{ mg/g}$  at pH 4.5, 6, and 4.5 for  $\text{Pb}^{2+}$ ,  $\text{Cd}^{2+}$ , and  $\text{Zn}^{2+}$ , respectively. The pH effect on ion adsorption by keratin powder can be explained based on  $\text{pH}_{\text{ZPC}}$  (4.3). The change in the adsorbed quantity within the studied pH range is due to the fact that at pH values higher than  $\text{pH}_{\text{ZPC}}$  the surface of keratin powder is negatively charged, whereas the metal ions are positively charged. At low pH, the solution contains a large number of  $\text{H}^+$  ions, which leads to a protonation effect, as demonstrated by the following expressions:

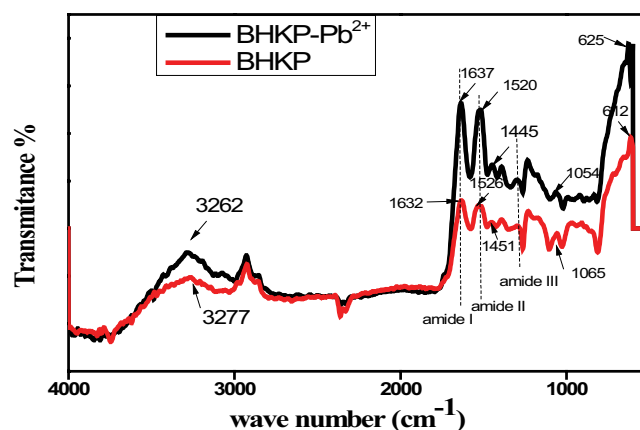
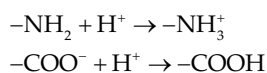


Fig. 2. Fourier-transform infrared spectroscopy characterization of BKASH biosorbent before and after  $\text{Pb}^{2+}$  ions sorption.

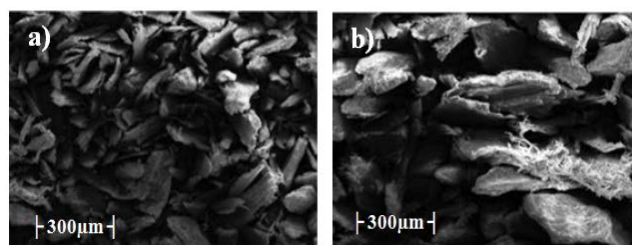


Fig. 3. Scanning electron microscopy images of BKASH: (a) before and (b) after  $\text{Pb}^{2+}$  ions sorption.

Therefore, the keratin surface and ion metals are positively charged under highly acidic conditions. With increasing pH values, the protonation degree of keratin biosorbent was reduced, and the electrostatic repulsion between keratin powder and metal ions was weakened, which resulted in the rapid increase of the adsorption capacity due to the electrostatic attraction between the active group and  $\text{Pb}^{2+}$ ,  $\text{Zn}^{2+}$  and  $\text{Cd}^{2+}$  ions. A similar trend was reported in the literature for various other biosorbents [36,37].

#### 3.2.2. Effect of adsorbent dosage

The effect of BKASH dosages on the biosorption capacity of  $\text{Pb}^{2+}$ ,  $\text{Cd}^{2+}$ , and  $\text{Zn}^{2+}$  ions was examined by varying the dosage from 0.02 to 1 g of biosorbent at an initial ions concentration of  $20\text{ mg/L}$  and an agitation speed of  $300\text{ rpm}$  at  $298\text{ K}$ . The results are presented in Fig. 5. The removal efficiency increased as the biosorbent loading increased up to 1 g, while the adsorption capacity decreased. This was due to the fact that more adsorbent addition created more adsorption points for ions, which was good for the overall removal result, but the adsorption chance for the unit area decreased, which was bad for the adsorption capacity. Additionally, more adsorbent can lead to larger resistance in the transportation process between adsorbent and adsorbents, and the electrostatic repulsion between them is also enhanced. Similar observations were reported for the removal of heavy metals using keratin as a biosorbent [38–41]. On considering this fact for the subsequent studies, the adsorbent dose was taken as 0.05 g.

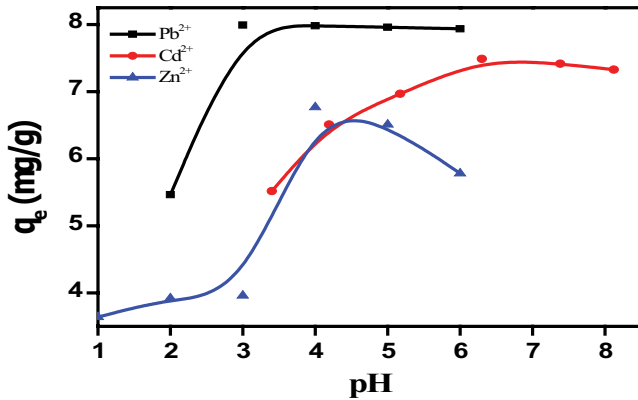


Fig. 4. Effect of pH on removal of  $Pb^{2+}$ ,  $Cd^{2+}$  and  $Zn^{2+}$  onto BKASH. ( $C_0 = 20$  mg/L,  $T = 298$  K).

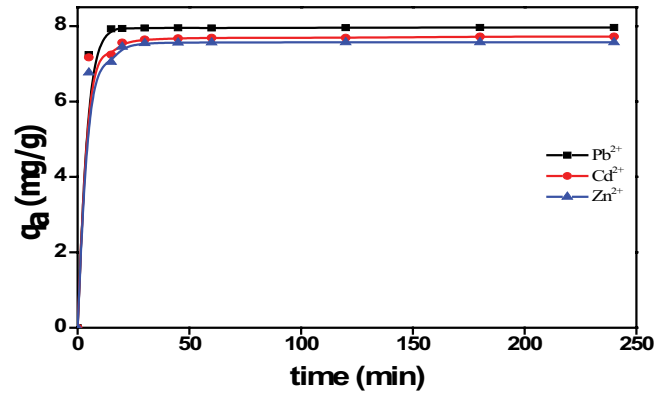


Fig. 6. Kinetics of adsorption of  $Cd^{2+}$ ,  $Pb^{2+}$  and  $Zn^{2+}$  onto BKASH ( $C_0 = 20$  mg/L,  $T = 298$  K,  $m_{\text{adsorbent}} = 0.05$  g).

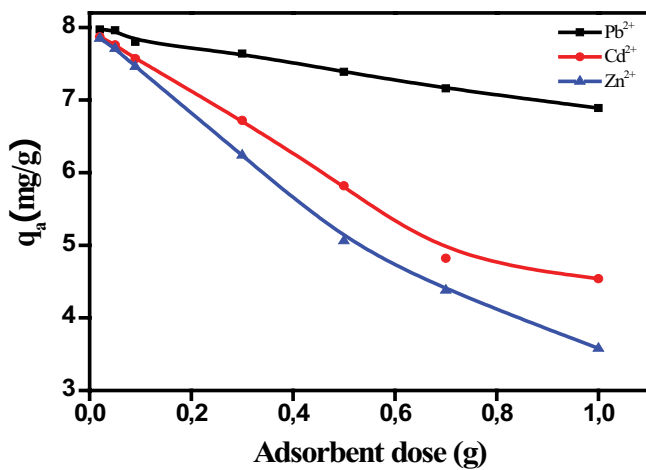


Fig. 5. Effect of adsorbent dosage on removal of  $Pb^{2+}$ ,  $Cd^{2+}$  and  $Zn^{2+}$  onto BKASH ( $C_0 = 20$  mg/L,  $T = 289$  K).

### 3.2.3. Effect of contact time

The adsorption kinetics of  $Cd^{2+}$ ,  $Pb^{2+}$ , and  $Zn^{2+}$  ions on tested BKASH were examined by using initial concentrations of 20 g/L at 298 K and pH values of 6, 4.5, and 4.5, respectively, as shown in Fig. 6. The results indicate that there was a rapid removal of ions within the first 10 min, with more than 80% of the removal of  $Pb^{2+}$ ,  $Cd^{2+}$ , and  $Zn^{2+}$  occurring within this period. The biosorption rate increased until equilibrium was attained after 30 min of agitation. Therefore, an equilibration time of 30 min was used for further experiments. The high initial biosorption rate is likely linked to the abundance of free binding sites on the biosorbent, which become saturated, resulting in a decreased biosorption rate.

The optimum adsorption capacity ( $q_{\text{max}}$ ) was 7.96, 7.7, and 7.57 mg/g of  $Pb^{2+}$ ,  $Cd^{2+}$ , and  $Zn^{2+}$ , respectively, with the optimum percentage removal being 99.4%, 94.2%, and 92.6% for  $Pb^{2+}$ ,  $Cd^{2+}$ , and  $Zn^{2+}$ , respectively (as shown in Fig. 7).

### 3.2.4. Effect of initial concentration and temperature

The adsorption isotherm of BKASH was used to analyze the interface adsorption behavior of  $Pb^{2+}$ ,  $Cd^{2+}$ , and

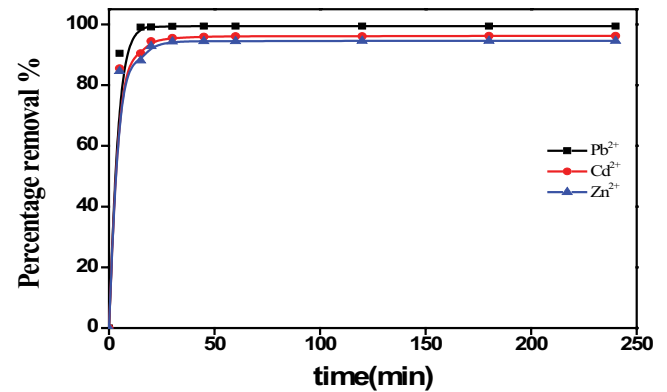


Fig. 7. Effect of contact time of the percentage removal of  $Cd^{2+}$ ,  $Pb^{2+}$  and  $Zn^{2+}$  onto BKASH ( $C_0 = 20$  mg/L,  $T = 298$  K,  $m_{\text{adsorbent}} = 0.05$  g).

$Zn^{2+}$  on the biosorbent. As shown in Fig. 8, the amount of  $Pb^{2+}$ ,  $Cd^{2+}$ , and  $Zn^{2+}$  adsorbed by BKASH increased as the initial concentration of ions ranged from 0 to 100 mg/L. The BKASH has significant potential for practical applications.

Furthermore, it was observed that the adsorption capacity of ions increased with a rise in temperature within the range of 287–313 K. As mentioned earlier, the problem removal rate also increased with temperature. This can be attributed to the higher mobility of  $Cd^{2+}$ ,  $Pb^{2+}$ , and  $Zn^{2+}$  ions toward the biosorbent at higher temperatures. Additionally, the activation of the surface and an increase in the biosorbent's pore size at high temperatures favor an increase in biosorption capacity [42].

### 3.3. Equilibrium isotherm

The Langmuir isotherm model, valid for monolayer adsorption on a homogeneous surface with equally available adsorption sites and without interactions between adsorbed species, is described by the following linearized equation:

$$\frac{C_e}{q_e} = \frac{1}{q_{\text{max}}} C_e + \frac{1}{K_L q_{\text{max}}} \quad (7)$$

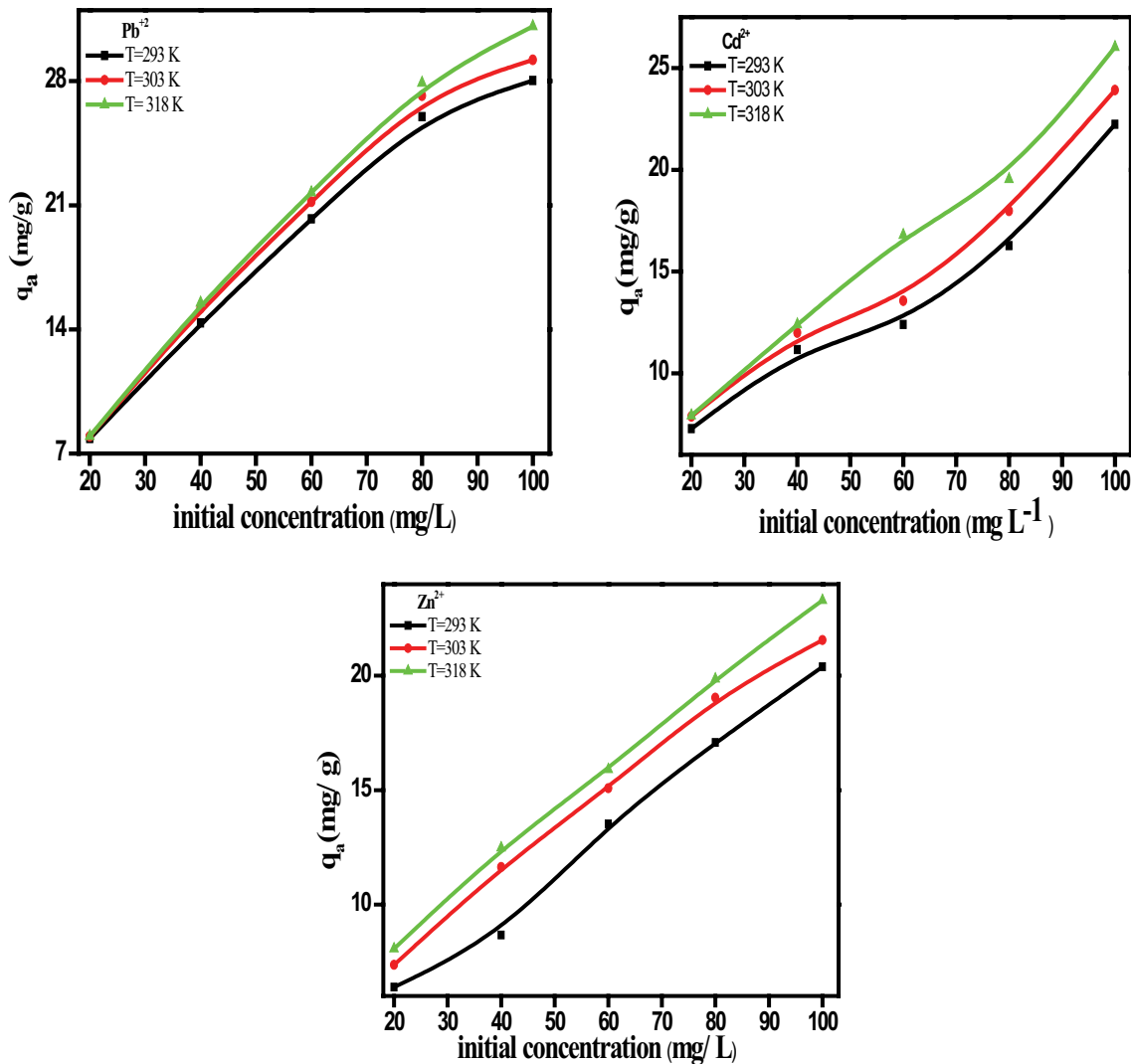


Fig. 8. Effect of initial concentration and temperature of the removal of Cd<sup>2+</sup>, Pb<sup>2+</sup> and Zn<sup>2+</sup> onto BKASH ( $C_0 = 20 \text{ mg/L}$ , contact time 30 min,  $m_{\text{adsorbent}} = 0.05 \text{ g}$ ).

where  $C_e$  is the equilibrium concentration (mg/L),  $q_e$  is the amount adsorbed at equilibrium time (mg/g), and  $q_{\text{max}}$  the maximum adsorption capacity and  $K_L$  is Langmuir constants related to energy (L/mg).

The  $q_{\text{max}}$ ,  $K_L$ , and correlation coefficient  $R^2$  obtained by fitting the experimental data Fig. 9 with the Langmuir equation are reported in Table 2.

Moreover, the dimensionless constant separation factor  $R_L$  was calculated in order to test the favorability of adsorption. The separation factor  $R_L$  is defined by the following equation:

$$R_L = \frac{1}{1 + K_L C_0} \tag{8}$$

where  $K_L$  is the Langmuir constant and  $C_0$  is the initial concentration (mg/L).  $R_L$  indicates whether the adsorption is favorable ( $0 < R_L < 1$ ) or unfavorable ( $R_L > 1$ ), linear ( $R_L = 1$ ), or irreversible ( $R_L = 0$ ).

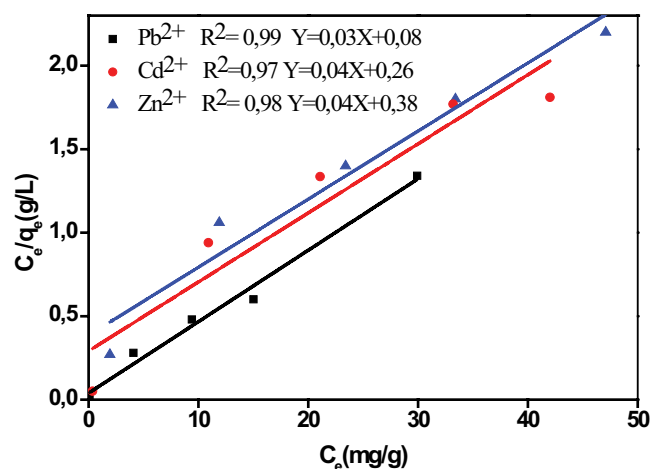


Fig. 9. Langmuir isotherm model for the adsorption of Cd<sup>2+</sup>, Pb<sup>2+</sup> and Zn<sup>2+</sup> onto BKASH.

Table 2  
Isotherm parameters for the removal of Pb<sup>2+</sup>, Cd<sup>2+</sup> and Zn<sup>2+</sup> ions adsorption on BKASH

Model	Langmuir	Freundlich	Temkin	Elovich
Pb <sup>2+</sup>	$q_{\max} = 33.33 \text{ mg/g}$ $K_L = 0.37$	$K_F = 12.35 \text{ mg/g}$ $1/n = 0.19$	$B_T = 2.94 \text{ mg/g}$ $B_T \ln(A_T) = 14$ $A_T = 138.37$ $\Delta Q = 1,238.19 \text{ J/mol}$	$q_{\max} = 5.02 \text{ mg/g}$ $K_e = 34.46 \text{ L/mg}$
R <sup>2</sup>	0.99	0.96	0.91	0.90
RMSE	10.8241	13.4123	15.2145	15.7612
$\chi^2$	1.002	2.123	3.621	3.826
Cd <sup>2+</sup>	$q_{\max} = 23.81 \text{ mg/g}$ $K_L = 0.16$	$K_F = 8.92 \text{ mg/g}$ $1/n = 0.2$	$B_T = 2.64 \text{ mg/g}$ $B_T \ln(A_T) = 9.1$ $A_T = 31.18$ $\Delta Q = 938.02 \text{ J/mol}$	$q_{\max} = 4.85 \text{ mg/g}$ $K_e = 6.76 \text{ L/mg}$
R <sup>2</sup>	0.97	0.92	0.88	0.88
RMSE	2.8141	6.4214	9.1545	9.6510
$\chi^2$	0.366	0.6452	1.1025	1.1810
Zn <sup>2+</sup>	$q_{\max} = 25 \text{ mg/g}$ $K_L = 0.1$	$K_F = 5.47 \text{ mg/g}$ $1/n = 0.33$	$B_T = 4.34$ $B_T \ln(A_T) = 3.23$ $A_T = 2.10$ $\Delta Q = 570.07 \text{ J/mol}$	$q_{\max} = 7.67 \text{ mg/g}$ $K_e = 0.9 \text{ L/mg}$
R <sup>2</sup>	0.98	0.97	0.96	0.93
RMSE	5.6251	6.0125	6.12	6.2412
$\chi^2$	0.465	0.861	1.0125	0.5645

The Freundlich isotherm model, which describes the adsorption process on energetically heterogeneous surfaces and is applicable when the amount of adsorbed solute increases indefinitely with the concentration of solute in the starting solution, can be described by the following linearized equation:

$$\ln q_e = \ln K_F + \frac{1}{n} \ln C_e \quad (9)$$

where  $K_F$  the adsorption capacity of the adsorbent (L/g) and  $n$  is an empirical give an indication of the adsorption favorability. The  $K_F$ ,  $n$ , and correlation coefficient  $R^2$  obtained by fitting the experimental data with the Freundlich equation are shown in Table 4. In particular, an  $n$  value falling between 1 and 10 indicates a favorable adsorption.

The Temkin isotherm assumes that the adsorption is characterized by a uniform distribution of binding energies, up to some maximum binding energy. This isotherm describes the behavior of adsorption systems on heterogeneous surfaces, and is applied in the following:

$$q_e = B_T \ln C_e + B_T \ln C_e \quad (10)$$

The adsorption data are analyzed according to Eq. (10). Therefore, the plot vs.  $q_e$  vs.  $\ln C_e$  enables to determine the constants  $A_T$  and  $B_T$ .

The Elovich isotherm is based on the principle of the kinetic, assuming that the number of adsorption sites augments exponentially with the adsorption; this implies a multilayer adsorption described by:

$$\ln \frac{q_e}{C_e} = \ln(q_{\max} K_e) - \frac{q_e}{q_{\max}} \quad (11)$$

where  $K_e$  (L/mg) is the Elovich constant at equilibrium,  $q_{\max}$  (mg/g) the maximum adsorption capacity,  $q_e$  (mg/g) the adsorption capacity at equilibrium, and  $C_e$  (mg/L) the concentration of the adsorbate at equilibrium. Both the equilibrium constant and maximum capacity is calculated from the plot of  $\ln(q_e/C_e)$  vs.  $q_e$ . The constants of the different models deduced after modeling are grouped in Table 2.

A critical examination of the correlation coefficients ( $R^2$ ), RMSE and the chi-square statistic ( $\chi^2$ ) shows that the Langmuir isotherm model ( $R^2 = 0.99$ ) had the highest correlation coefficient compared to the other three isotherm models. The  $\chi^2$  and RMSE values for Langmuir model were 0.1002 and 1.8241, respectively, which were lower than all other isotherm models. This suggests that the adsorption process was monolayer adsorption, indicating good homogeneity of the sponge surface. The maximum adsorption capacities ( $q_{\max}$ ) calculated from the Langmuir equation at 298 K were 33.33, 23.83, and 25 mg/g for Pb<sup>2+</sup>, Cd<sup>2+</sup>, and Zn<sup>2+</sup>, respectively. The  $R_L$  values of the ions for BKASH are plotted against the initial metal ion concentration Fig. 10. As shown, for all the considered initial metal ion concentrations, the  $R_L$  values fall between 0 and 1, indicating favorable adsorption of Pb<sup>2+</sup>, Cd<sup>2+</sup>, and Zn<sup>2+</sup> ions on BKASH.

From the Freundlich isotherm fitting results, the values of  $1/n$  obtained from this study were found to be 0.19 for Pb<sup>2+</sup>, 0.2 for Cd<sup>2+</sup>, and 0.33 for Zn<sup>2+</sup>, indicating favorable adsorption of all heavy metals on BKASH. Additionally,

the Freundlich isotherm does not predict the saturation of heavy metal ions on the surface of the adsorbent and thus reinforces the infinite coverage of the adsorbent surface. The change in adsorption energy for the Temkin isotherm is positive, indicating the endothermic nature of adsorption of metal ions by BKASH.

As shown in Table 2, the values of the regression coefficient  $R^2$  are low; therefore, the adsorption of  $\text{Cd}^{2+}$ ,  $\text{Pb}^{2+}$ , and  $\text{Zn}^{2+}$  onto BKASH does not fit the Elovich isotherm.

### 3.4. Kinetic studies

The adsorption kinetics of the biosorption of  $\text{Cd}^{2+}$ ,  $\text{Pb}^{2+}$  and  $\text{Zn}^{2+}$  ions, were analysed using Lagergren first-order and Lagergren second-order kinetic models and intra-particle diffusion. The Lagergren first-order equation is expressed as follows:

$$\log(q_e - q_t) = \log q_e - \frac{K_1}{2.303} t \quad (12)$$

where  $q_e$  and  $q_t$  (mg/g) are the adsorption capacity at equilibrium and at time  $t$ , respectively, and  $K_1$  is the Lagergren rate constant of the pseudo-first-order adsorption (L/min).

A plot of  $\log(q_e - q_t)$  vs.  $t$  (Fig. 11) gave a straight line confirming the applicability of the Lagergren first-order rate equation.  $K_1$  and  $q_e$  can be determined from the slope and intercept of the plot, respectively. Lagergren second-order sorption rate equation can be expressed as:

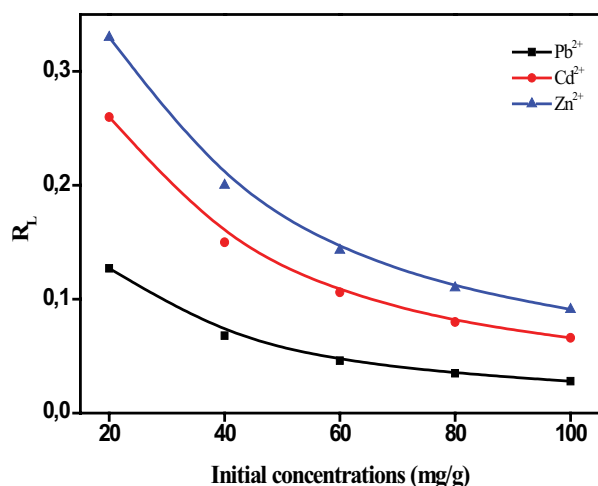


Fig. 10. Separation factor for the adsorption of  $\text{Cd}^{2+}$ ,  $\text{Pb}^{2+}$  and  $\text{Zn}^{2+}$  onto BKASH.

$$\frac{t}{q_t} = \frac{1}{k_2 q_e^2} + \frac{1}{q_e} t \quad (13)$$

where  $K_2$  is the rate constant of the pseudo-second-order adsorption (g/mg·min).

A straight-line plot of  $t/q_t$  vs. time in Fig. 12 indicates the applicability of second-order model.

The rate constants  $K_1$ ,  $K_2$  and the calculated equilibrium adsorption capacity  $q_{e,cal}$  from first-order and second-order equations, and the experimental equilibrium adsorption capacity  $q_{e,exp}$  (mg/g) are presented in Table 3.

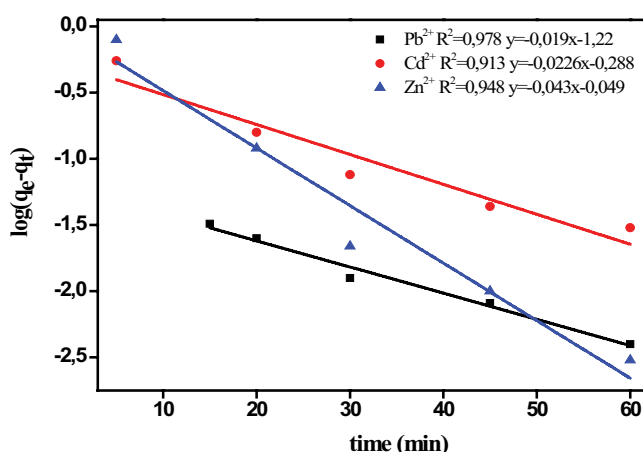


Fig. 11. Pseudo-first-order kinetic plot for the adsorption of  $\text{Cd}^{2+}$ ,  $\text{Pb}^{2+}$  and  $\text{Zn}^{2+}$  onto BKASH.

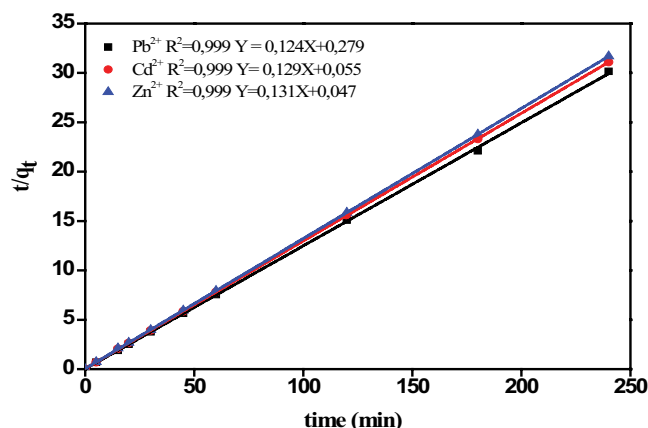


Fig. 12. Pseudo-second-order kinetic plot for the adsorption of  $\text{Cd}^{2+}$ ,  $\text{Pb}^{2+}$  and  $\text{Zn}^{2+}$  onto BKASH.

Table 3  
Kinetic parameters for metal adsorption onto BKASH at 298°K

Metal	$C_0$ (mg/L)	$q_{e,exp}$ (mg/g)	Pseudo-first-order kinetic			Pseudo-second-order kinetic			
			$K_1$ (min <sup>-1</sup> )	$q_e$ (mg/g)	$R^2$	$K_2$ (g/mg·min)	$q_e$ (mg/g)	$R^2$	$\Delta q/q$ %
$\text{Pb}^{2+}$	20	7.96	0.046	0.06	0.98	0.06	8.01	0.99	0.6
$\text{Cd}^{2+}$	20	7.72	0.66	0.95	0.91	0.3	7.75	0.99	0.6
$\text{Zn}^{2+}$	20	7.60	0.11	0.89	0.95	0.35	7.63	0.99	0.4

The high correlation coefficient in the pseudo-second-order plot for all metals confirms that the adsorption reaction follows the pseudo-second-order kinetic model, unlike the pseudo-first-order plots, which are not applicable to the present system. The  $q_{e,cal}$  obtained from the pseudo-second-order model shows good agreement with the experimental data. This suggests that the adsorption of metal ions involves a chemical reaction (chemisorption), including an exchange of electrons between the adsorbent and the adsorbate, resulting in the attachment of metal ions to the adsorbent surface by chemical bonding.

BKASH exhibits an ion biosorption capacity that is comparable to the majority of adsorbents reported in the literature [43,44], making it an excellent candidate for use as a biosorbent to remove  $Cd^{2+}$ ,  $Pb^{2+}$ , and  $Zn^{2+}$  ions from aqueous solutions.

The diffusion mechanism controlling biosorption cannot be shown by the pseudo-first-order or pseudo-second-order models. Thus, Weber–Morris suggested that the intraparticle diffusion model can be used to analyze kinetic data in order to understand the diffusion effects. The general form of Weber's diffusion model is expressed as:

$$q_t = K_{id} \sqrt{t} + C \quad (14)$$

where  $K_{id}$  is the intraparticle diffusion rate constant ( $mg/g \cdot min^{1/2}$ ),  $q_t$  the amount of ions adsorbed at time  $t$  and  $C$  ( $mg/g$ ) is the intercept that relates to the thickness of the boundary layer.

The plots of  $q_t$  vs.  $t^{1/2}$  are shown in Fig. 13. The linear relation between  $q_t$  and  $t^{1/2}$  indicated the presence of intraparticle diffusion in the adsorption process.

Multi-linear correlations were observed in the plots, indicating that the biosorption process of heavy metals involves three distinct steps. Table 4 presents the parameters of the three linear portions of the Weber–Morris intraparticle diffusion model, which were evaluated for the adsorption of  $Cd^{2+}$ ,  $Pb^{2+}$ , and  $Zn^{2+}$  ions on the BKASH adsorbent. The values of  $K_{id}$  in the first step were all higher than those in the second step. The first linear portion corresponds to the initial, rapid adsorption stage, where the rate of metal

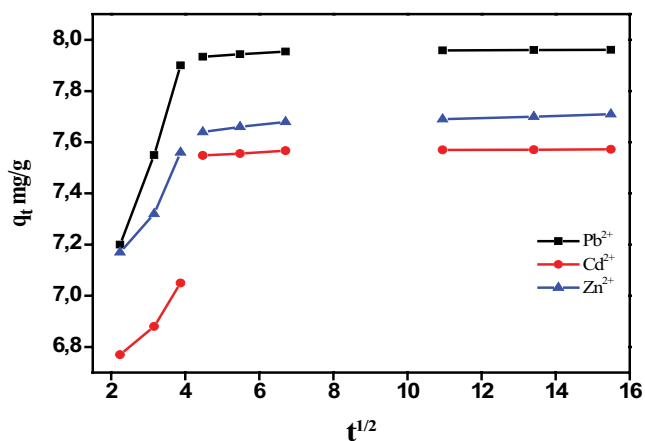


Fig. 13. Intraparticle diffusion plots for adsorption of  $Cd^{2+}$ ,  $Pb^{2+}$  and  $Zn^{2+}$  onto BKASH.

ions onto the surface of the BKASH adsorbent was high due to Van der Waal's forces. In the second step, the metal ions are transported to the external surface of the BKASH adsorbent through film diffusion, that is, intraparticle diffusion occurs in the initial stage, while film biosorption occurs in the second stage. The third step represents the equilibrium state, where intraparticle diffusion is constant. Furthermore, the fact that  $C \neq 0$  and that the fitted straight line did not pass through the origin of coordinates indicate that the diffusion process was not the rate-controlling step.

In summary, the kinetic studies showed that the adsorption process of  $Pb^{2+}$ ,  $Cd^{2+}$ , and  $Zn^{2+}$  by BKASH is quite complex, consisting of both surface adsorption and intraparticle diffusion. Intraparticle diffusion controls the early stage, while chemical sorption plays the main role in the sorption process as a whole.

### 3.5. Performances of the prepared BKASH

Table 5 presents a comparison of the percentage removal of heavy metal ions using various keratin materials reported in the literature, as well as BKASH. It should be noted that direct comparison of adsorption capacities between different biosorbents is challenging due to variations in experimental conditions. Nonetheless, BKASH showcased an exceptionally high efficacy in removing heavy metal ions, all achieved without the need for any additional treatments. In particular, BKASH achieved removal percentages of up to 92% for  $Pb^{2+}$ ,  $Cd^{2+}$ , and  $Zn^{2+}$ , which is significantly higher than the removal percentages achieved by treated adsorbents (ranging from 41% to 87%). The superior performance of BKASH can be attributed to its natural properties, such as high surface area, high concentration of functional groups, and excellent stability. BKASH was prepared without any physical or chemical treatments to maintain its natural properties, which may contribute to its higher adsorption capacity and selectivity.

### 3.6. Determination of thermodynamic parameters

The insights of the adsorption mechanism can be determined from the thermodynamic parameters namely free energy ( $\Delta G^\circ$ ), enthalpy ( $\Delta H^\circ$ ) and entropy ( $\Delta S^\circ$ ). This thermodynamic parameters are determined from the following equations.

Table 4  
Parameters of the Weber–Morris intraparticle diffusion model

Ions	Step	$K_{id}$ ( $mg/g \cdot min^{1/2}$ )	$C_i$ ( $mg/g$ )	$R^2$
$Pb^{2+}$	1	0.42	6.23	0.98
	2	0.0089	7.89	0.99
	3	$4.4 \times 10^{-4}$	7.95	0.99
$Cd^{2+}$	1	0.04	7.07	0.99
	2	0.017	7.56	0.99
	3	0.004	7.64	0.99
$Zn^{2+}$	1	0.26	6.4	0.92
	2	0.0085	7.5	0.99
	3	$4.4 \times 10^{-4}$	7.56	0.99

Table 5  
Removal of metal ions by different forms of keratin materials

Keratin-based adsorbents	Metal ions	Percentage removal (%)	References
Chemically treated human hair	Pb <sup>2+</sup>	96	[24]
	Cd <sup>2+</sup>	86	
Cow hooves	Pb <sup>2+</sup>	96.2	[38]
Duck feather (adhesive bonded)	Cu <sup>2+</sup>	41	[45]
Wool-derived keratin nanofiber membranes	Cu <sup>2+</sup>	95	[46]
	Ni <sup>2+</sup>	65	
	Co <sup>2+</sup>	59	
Chemically treated sheep wool	Cu <sup>2+</sup>	99	[47]
Wool keratin/PET composite nanofiber	Cr <sup>3+</sup>	75.86	[48]
Colloidal keratin solution obtained from wool	Pb <sup>2+</sup>	87	[49]
Algerian sheep hoof powder	Pb <sup>2+</sup>	65	[50]
	Cd <sup>2+</sup>	70	
	Zn <sup>2+</sup>	65	
Algerian sheep horns powder	Pb <sup>2+</sup>	99.4	This works
	Cd <sup>2+</sup>	96.2	
	Zn <sup>2+</sup>	94.6	

$$\Delta G^\circ = -RT \ln K_e \tag{15}$$

$$\Delta G^\circ = \Delta H^\circ - T\Delta S^\circ \tag{16}$$

$$K_e = \frac{C_0 - C_e}{C_0} \tag{17}$$

$$\ln K_e = -\frac{\Delta H^\circ}{RT} + \frac{\Delta S^\circ}{R} \tag{18}$$

where  $K_e$  is the equilibrium constant,  $R$  is the gas constant (8.314 J/mol·K), and  $T$  is the temperature (K). The values of  $\Delta H^\circ$  and  $\Delta S^\circ$  are determined from the slope and the intercept of the plots of  $\ln K_e$  vs.  $1/T$  (Fig. 14). The  $\Delta G^\circ$  values were calculated using Eq. (12). The plots were used to compute the values of thermodynamic parameters (Table 6).

The biosorption of Cd<sup>2+</sup>, Pb<sup>2+</sup>, and Zn<sup>2+</sup> on BKASH is a spontaneous process, as indicated by the negative value of  $\Delta G^\circ$ . A more negative  $\Delta G^\circ$  value indicates a more energetically favorable adsorption process. Furthermore, the decrease in free energy values with increasing temperature from 287 to 318 K suggests that the adsorption process becomes more feasible at higher temperatures. The positive values of  $\Delta H^\circ$  for all metal ions indicate that the adsorption is endothermic, which is supported by the increased metal uptake with a rise in temperature. The magnitude of  $\Delta H^\circ$  provides insight into the type of sorption, whether physical or chemical. Typically, the enthalpy for physical adsorption is no more than 1 kcal/mol (4.2 kJ/mol), while for chemical adsorption, it is more than 5 kcal/mol (21 kJ/mol) [51]. Therefore, the adsorption of Mn<sup>+</sup> ions on BKASH appears to be primarily a chemical process, with strong interactions between the Mn<sup>+</sup> ions and the functional groups on the adsorbent's surface. The positive  $\Delta S^\circ$  value indicates that the sorbed ions are unstable on the biosorbent surface, which

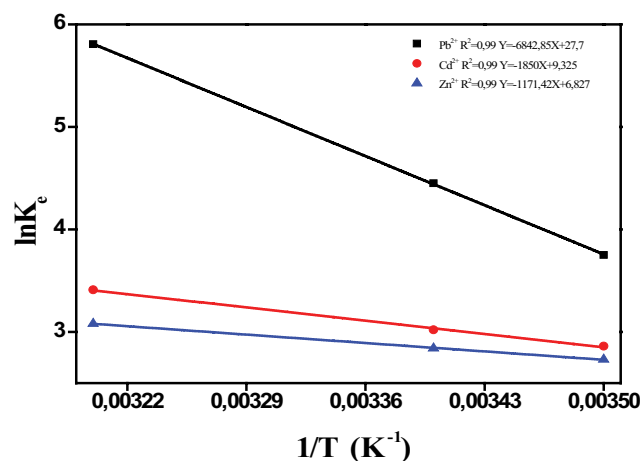


Fig. 14. Thermodynamic parameters, enthalpy and entropy for the adsorption of Cd<sup>2+</sup>, Pb<sup>2+</sup> and Zn<sup>2+</sup> ions onto BKASH.

Table 6  
Thermodynamic parameters for the adsorption of Pb<sup>2+</sup>, Cd<sup>2+</sup> and Zn<sup>2+</sup> ions onto BKASH

	$\Delta H^\circ$ (kJ/mol·K)	$\Delta S^\circ$ (J/mol·K)	$\Delta G^\circ$ (kJ/mol)		
			287 K	297 K	318 K
Pb <sup>2+</sup>	56.7	230.38	-2.96	-10.99	-15.35
Cd <sup>2+</sup>	15.38	77.53	-6.82	-7.46	-9.015
Zn <sup>2+</sup>	15.08	76.24	-6.51	-7.012	-8.14

suggests an increased randomness at the solid solution interface during metal ion adsorption. These types of biosorption behavior have also been observed by other researchers [52–54].

### 3.7. Adsorption mechanisms

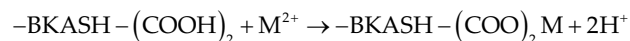
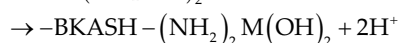
The isotherm and kinetics analyses suggest that chemisorption and intraparticle diffusion are critical mechanisms in the adsorption process, but other mechanisms may also contribute to the process.

When discussing the adsorption mechanisms of  $Pb^{2+}$ ,  $Zn^{2+}$ , and  $Cd^{2+}$  onto biosorbents, it is important to consider the functional groups and surface chemical properties. Various scientists have proposed mechanisms based on assumptions and empirical results, such as ion exchange, surface precipitation or complexation, electrostatic attraction, and physical adsorption. Among these, ion exchange is the most significant hypothesized process for comprehending and interpreting the biosorption mechanism. Protons and metallic cations, two positively charged species present in waste solutions, compete for binding sites under the strong influence of pH, which is considered a major factor in this process [55].

Studies have shown that keratin primarily uses its carboxylic and amino groups to bind with heavy metal cations in aqueous solutions [56–58]. FTIR spectra of BKASH indicated that the hydroxyl, carboxylate, amino and thiol groups are involved in the adsorption process. The BKASH has a thiol (SH) group that is very reactive with cadmium, zinc, and lead to form a very stable complex.

The high affinity of Cd, Zn, and Pb for the thiol (SH) group suggests that at the first moments of contact between the BKASH and the solution, a quantity of metal is captured by the thiol functions in a short time [50]. This result was already observed with the adsorption of  $Pb^{2+}$ ,  $Zn^{2+}$ , and  $Cd^{2+}$  using steamed Algerian sheep hoof powder in our previous study. The speed of adsorption in the first moments of the test allows us to infer that the adsorption occurs on the outer surface of the adsorbent grains.

The adsorption of heavy metal ions on BKASH surfaces can be represented by the following expressions:



## 4. Conclusion

This study presents a novel application of keratinous materials derived from bioresources for the removal of heavy metals, specifically using Algerian sheep horns to prepare brut keratin powder, which was found to be an effective biosorbent for removing  $Pb^{2+}$ ,  $Cd^{2+}$ , and  $Zn^{2+}$  ions from wastewater. The optimum pH for the uptake of  $Pb^{2+}$ ,  $Cd^{2+}$ , and  $Zn^{2+}$  was determined to be 4.5, 6, and 4.5, respectively, and rapid removal was observed without lengthy agitation times, with an optimum contact time of 30 min. The removal effectiveness was determined to be 99% for  $Pb^{2+}$ , 94% for  $Zn^{2+}$ , and 96% for  $Cd^{2+}$  using 0.05 g of biosorbent and 20 mg/L of initial ion concentration. Equilibrium data were tested using Langmuir, Freundlich, Temkin, and Elovich isotherms. The Langmuir isotherm was found to

be well-fitted to the experimental data, and the adsorption rate of heavy metal ions was fast. This confirmed that the mechanism of sorption occurred at specific sites. The kinetics of  $Pb^{2+}$ ,  $Cd^{2+}$ , and  $Zn^{2+}$  ion adsorption on powder keratin were investigated using pseudo-second-order kinetic models, which rely on the assumption that chemisorption is the rate-limiting step. The intraparticle diffusion model indicates that the external surface adsorption (stage 1) is absent because of completing before 5 min, and final equilibrium adsorption (stage 3) is started after 30 min. The  $Pb^{2+}$ ,  $Cd^{2+}$ , and  $Zn^{2+}$  is transported via intraparticle diffusion into the particles and is finally retained in micropores. The negative value of  $\Delta G^\circ$  and positive value of  $\Delta S^\circ$  indicated that adsorption was spontaneous and feasible. The positive value of  $\Delta H^\circ$  confirmed the endothermic nature of adsorption. The FTIR spectrum of the keratin before and after adsorption exhibited different functional groups, such as carboxyl, amino, and hydroxyl groups. FTIR and SEM analysis also explained the adsorption mechanisms including electrostatic interaction and ion-exchange with the action of functional groups, such as  $-COOH$ ,  $-NH_2$  and  $-S-SH$ . Based on the results, it can be concluded that waste brut keratin powder can be reprocessed into effective biosorbents for removing  $Pb^{2+}$ ,  $Cd^{2+}$ , and  $Zn^{2+}$  ions from aqueous solutions. The adsorbent is natural, non-toxic, and has the potential to be a cost-effective alternative to conventional methods of heavy metal removal.

## Funding

No funding received.

## Acknowledgements

This work was supported by The Algerian Petroleum Institute (Chemistry, Industrial Safety and Environment Department). The authors thank Dr. Aldjia Ait ouakli for technical assistance.

## Authors contribution

All authors contributed to the study. FS gave concept, designed and conducted the experimental work, and investigated and wrote the paper under the supervision of RS. NS analyzed experimental data. The manuscript was revised through discussion and comments of all the authors. All authors read and approved the final manuscript.

## Conflict of interest

The authors declare that they have no known competing financial interests or personal relationships that could have appeared to influence the work reported in this paper.

## References

- [1] A. Pugazhendhi, G.M. Boovaragamoorthy, K. Ranganathan, Mu. Naushad, T. Kaliannan, New insight into effective biosorption of lead from aqueous solution using *Ralstonia solanacearum*: characterization and mechanism studies, J. Cleaner Prod., 174 (2018) 1234–1239.

- [2] S.S. Ahluwalia, D. Goyal, Microbial and plant derived biomass for removal of heavy metals from wastewater, *Bioresour. Technol.*, 98 (2007) 2243–2257.
- [3] R.A.K. Rao, A. Khatoun, Aluminate treated *Casuarina equisetifolia* leaves as potential adsorbent for sequestering Cu(II), Pb(II) and Ni(II) from aqueous solution, *J. Cleaner Prod.*, 165 (2017) 1280–1295.
- [4] S.L. Cardoso, C.S.D. Costa, E. Nishikawa, M.G.C. da Silva, M.G.A. Vieira, Biosorption of toxic metals using the alginate extraction residue from the brown algae *Sargassum filipendula* as a natural ion-exchanger, *J. Cleaner Prod.*, 165 (2017) 491–499.
- [5] P.B. Tchounwou, C.G. Yedjou, A.K. Patlolla, D.J. Sutton, Heavy metal toxicity and the environment, *Exp. Suppl.*, 101 (2012) 133–164.
- [6] Q. Chen, Z. Luo, C. Hills, G. Xue, M. Tyrer, Precipitation of heavy metals from wastewater using simulated flue gas: sequent additions of fly ash, lime and carbon dioxide, *Water Res.*, 43 (2009) 2605–2614.
- [7] F. Fu, L. Xie, B. Tang, Q. Wang, S. Jiang, Application of a novel strategy—advanced Fenton-chemical precipitation to the treatment of strong stability chelated heavy metal containing wastewater, *Chem. Eng. J.*, 189–190 (2012) 283–287.
- [8] T. Bakalár, M. Búgel, L. Gajdošová, Heavy metal removal using reverse osmosis, *Acta Montan. Slovaca*, 14 (2009) 250–253.
- [9] M.A. Barakat, E. Schmidt, Polymer-enhanced ultrafiltration process for heavy metals removal from industrial wastewater, *Desalination*, 256 (2010) 90–93.
- [10] P. Shah, C.N. Murthy, Studies on the porosity control of MWCNT/polysulfone composite membrane and its effect on metal removal, *J. Membr. Sci.*, 437 (2013) 90–98.
- [11] G. Al-Enezi, M.F. Hamoda, N. Fawzi, Ion exchange extraction of heavy metals from wastewater sludges, *J. Environ. Sci. Health. Part A Toxic/Hazard. Subst. Environ. Eng.*, 39 (2004) 455–464.
- [12] H.A. Qdais, H. Moussa, Removal of heavy metals from wastewater by membrane processes: a comparative study, *Desalination*, 164 (2004) 105–110.
- [13] C. Londono-Zuluaga, H. Jameel, R.W. Gonzalez, L. Lucia, Crustacean shell-based biosorption water remediation platforms: status and perspectives, *J. Environ. Manage.*, 231 (2019) 757–762.
- [14] E. Koohzad, D. Jafari, H. Esmaeili, Adsorption of lead and arsenic ions from aqueous solution by activated carbon prepared from tamarix leaves, *Chem. Select*, 4 (2019) 12356–12367.
- [15] W.S. Wan Ngah, S. Fatinathan, Pb(II) biosorption using chitosan and chitosan derivatives beads: equilibrium, ion exchange and mechanism studies, *J. Environ. Sci.*, 22 (2010) 338–346.
- [16] D. Sud, G. Mahajan, M.P. Kaur, Agricultural waste material as potential adsorbent for sequestering heavy metal ions from aqueous solutions – a review, *Bioresour. Technol.*, 99 (2008) 6017–6027.
- [17] P. Kar, M. Misra, Use of keratin fiber for separation of heavy metals from water, *J. Chem. Technol. Biotechnol.*, 79 (2004) 1313–1319.
- [18] H. Zhang, F. Carrillo, M. López-Mesas, C. Palet, Valorization of keratin biofibers for removing heavy metals from aqueous solutions, *Text. Res. J.*, 89 (2019) 1153–1165.
- [19] Z. Sfaksi, N. Azzouz, A. Abdelwahab, Removal of Cr(VI) from water by cork waste, *Arabian J. Chem.*, 7 (2014) 37–42.
- [20] R. Naik, G. Wen, M.S. Dharmaprasanth, S. Hureau, A. Uedono, X. Wang, X. Liu, P.G. Cookson, S.V. Smith, Metal ion binding properties of novel wool powders, *J. Appl. Polym. Sci.*, 115 (2010) 1642–1650.
- [21] W. Kong, Q. Li, J. Liu, X. Li, L. Zhao, Y. Su, Q. Yue, B. Gao, Adsorption behavior and mechanism of heavy metal ions by chicken feather protein-based semi-interpenetrating polymer networks super absorbent resin, *RSC Adv.*, 6 (2016) 83234–83243.
- [22] A.S. Saini, J.S. Melo, Biosorption of uranium by human black hair, *J. Environ. Radioact.*, 142 (2015) 29–35.
- [23] B. Ma, X. Qiao, X. Hou, Y. Yang, Pure keratin membrane and fibers from chicken feather, *Int. J. Biol. Macromol.*, 89 (2016) 614–621.
- [24] H. Zhang, F. Carrillo-Navarrete, M. López-Mesas, C. Palet, Use of chemically treated human hair wastes for the removal of heavy metal ions from water, *Water*, 12 (2020): 1263, doi: 10.3390/w12051263.
- [25] S. Saha, M. Zubair, M.A. Khosa, S. Song, A. Ullah, Keratin and chitosan biosorbents for wastewater treatment: a review, *J. Polym. Environ.*, 27 (2019) 1389–1403.
- [26] M.R. Samarghandi, M. Hadi, S. Moayedi, F. Barjasteh Askari, Two-parameter isotherms of methyl orange sorption by pinecone derived activated carbon, *Iran. J. Environ. Health Sci. Eng.*, 6 (2009) 285–294.
- [27] S. Lagergren, About the theory of so-called adsorption of soluble substances, *Kungliga Svenska Vetenskapsakademiens, Handlingar*, 24 (1898) 1–39.
- [28] I. Langmuir, The adsorption of gases on plane surfaces of glass, mica and platinum, *J. Am. Chem. Soc.*, 40 (1918) 1361–1403.
- [29] H. Freundlich, Of the adsorption of gases. Section II. Kinetics and energetics of gas adsorption. Introductory paper to section II, *Trans. Faraday Soc.*, 28 (1932) 195–201.
- [30] M.J. Tempkin, V. Pyzhev, Kinetics of ammonia synthesis on promoted iron catalysts, *Acta Physicochim U.R.S.S.*, 12 (1940) 217–222.
- [31] T. Aksil, M. Abbas, M. Trari, S. Benamara, Water adsorption on lyophilized *Arbutus unedo* L. fruit powder: determination of thermodynamic parameters, *Microchem. J.*, 145 (2019) 35–41.
- [32] I.A. Aguayo-Villarreal, A. Bonilla-Petriciolet, V. Hernández-Montoya, M.A. Montes-Morán, H.E. Reynel-Avila, Batch and column studies of Zn<sup>2+</sup> removal from aqueous solution using chicken feathers as sorbents, *Chem. Eng. J.*, 167 (2011) 67–76.
- [33] G.C. Bassler, T.C. Morrill, *Spectroscopic Identification of Organic Compounds*, R.M. Silverstein, 4th ed., Wiley, New York, 1981, pp. 247–283.
- [34] G. Fadillah, E.N.K. Putri, S. Febrianastuti, E.V. Maylinda, C. Purnawan, Adsorption of Fe ions from aqueous solution using  $\alpha$ -keratin-coated alginate biosorbent, *Int. J. Environ. Sci. Dev.*, 9 (2018) 82–85.
- [35] S.A. Olawale, A. Bonilla-Petriciolet, D.I. Mendoza-Castillo, C.C. Okafor, L. Sellaoui, M. Badawi, Thermodynamics and mechanism of the adsorption of heavy metal ions on keratin biomasses for wastewater detoxification, *Adsorpt. Sci. Technol.*, 2022 (2022) 7384924, doi: 10.1155/2022/7384924.
- [36] H. Cao, X. Ma, Z. Wei, Y. Tan, S. Chen, T. Ye, M. Yuan, J. Yu, X. Wu, F. Yin, F. Xu, Behavior and mechanism of the adsorption of lead by an eco-friendly porous double-network hydrogel derived from keratin, *Chemosphere*, 289 (2022) 133086, doi: 10.1016/j.chemosphere.2021.133086.
- [37] P.L. Homagai, H. Paudyal, Adsorption kinetics of Pb(II), Cd(II), Zn(II) and Fe(III) onto saponified apple waste, *J. Nepal Chem. Soc.*, 23 (2009) 102–105.
- [38] I. Osasona, A.O. Adebayo, O.O. Ajayi, Biosorption of Pb(II) from aqueous solution using cow hooves: kinetics and thermodynamics, *ISRN Phys. Chem.*, 2013 (2013) 171865, doi: 10.1155/2013/171865.
- [39] R. Chakraborty, A. Asthana, A.K. Singh, S. Yadav, Md. A.B.H. Susan, S.A.C. Carabineiro, Intensified elimination of aqueous heavy metal ions using chicken feathers chemically modified by a batch method, *J. Mol. Liq.*, 312 (2020) 113475, doi: 10.1016/j.molliq.2020.113475.
- [40] Y. Zhuang, X.-X. Zhao, M.-H. Zhou, Cr(VI) adsorption on a thermoplastic feather keratin film, *Desal. Water Treat.*, 52 (2014) 2786–2791.
- [41] M. Dudyński, K. Kwiatkowski, K. Bajer, From feathers to syngas – technologies and devices, *Waste Manage.*, 32 (2012) 685–691.
- [42] E. Nakkeeran, N. Selvaraju, Biosorption of chromium(VI) in aqueous solutions by chemically modified Strachyline tree fruit shell, *Int. J. Phytorem.*, 19 (2017) 1065–1076.
- [43] V.S. Munagapati, V. Yarramuthi, S.K. Nadavala, S.R. Alla, K. Abburi, Biosorption of Cu(II), Cd(II) and Pb(II) by *Acacia leucocephala* bark powder: kinetics, equilibrium and thermodynamics, *Chem. Eng. J.*, 157 (2010) 357–365.
- [44] Z. Reddad, C. Gerente, Y. Andres, P. Le Cloirec, Adsorption of several metal ions onto a low-cost biosorbent: kinetic and equilibrium studies, *Environ. Sci. Technol.*, 36 (2002) 2067–2073.

- [45] X. Jin, L. Lu, H. Wu, Q. Ke, H. Wang, Duck feather/nonwoven composite fabrics for removing metals present in textile dyeing effluents, *J. Eng. Fibers Fabr.*, 8 (2013) 89–96.
- [46] A. Aluigi, A. Corbellini, F. Rombaldoni, G. Mazzuchetti, Wool-derived keratin nanofiber membranes for dynamic adsorption of heavy-metal ions from aqueous solutions, *Text. Res. J.*, 83 (2013) 1574–1586.
- [47] S. Enkhzaya, K. Shiomori, B. Oyuntsetseg, Effective adsorption of Au(III) and Cu(II) by chemically treated sheep wool and the binding mechanism, *J. Environ. Chem. Eng.*, 8 (2020) 104021, doi: 10.1016/j.jece.2020.104021.
- [48] X. Jin, H. Wang, X. Jin, H. Wang, L. Chen, W. Wang, T. Lin, Z. Zhu, Preparation of keratin/PET nanofiber membrane and its high adsorption performance of Cr(VI), *Sci. Total Environ.*, 710 (2020) 135546, doi: 10.1016/j.scitotenv.2019.135546.
- [49] Y. Sekimoto, T. Okiharu, H. Nakajima, T. Fujii, K. Shirai, H. Moriwaki, Removal of Pb(II) from water using keratin colloidal solution obtained from wool, *Environ. Sci. Pollut. Res.*, 20 (2013) 6531–6538.
- [50] S. Rafika, T. Djilali, B. Benchreit, B. Ali, Adsorption of heavy metals (Cd, Zn and Pb) from water using keratin powder prepared from Algerien sheep hoofs, *Eur. J. Sci. Res.*, 35 (2009) 416–425.
- [51] D. Ozdes, A. Gundogdu, B. Kemer, C. Duran, H.B. Senturk, M. Soylyak, Removal of Pb(II) ions from aqueous solution by a waste mud from copper mine industry: equilibrium, kinetic and thermodynamic study, *J. Hazard. Mater.*, 166 (2009) 1480–1487.
- [52] M. Marciniak, J. Goscianska, M. Frankowski, R. Pietrzak, Optimal synthesis of oxidized mesoporous carbons for the adsorption of heavy metal ions, *J. Mol. Liq.*, 276 (2019) 630–637.
- [53] K.M. Elsherif, A.M. Alkheraz, A.K. Ali, Removal of Pb(II), Zn(II), Cu(II) and Cd(II) from aqueous solutions by adsorption onto olive branches activated carbon: equilibrium and thermodynamic studies, *Chem. Int.*, 6 (2020) 11–20.
- [54] A. Babarinde, K. Ogundipe, K.T. Sangosanya, B.D. Akintola, A.-O. Elizabeth Hassan, Comparative study on the biosorption of Pb(II), Cd(II) and Zn(II) using Lemon grass (*Cymbopogon citratus*): kinetics, isotherms and thermodynamics, *Chem. Int.*, 2 (2016) 89–102.
- [55] A. Ahmad, A.H. Bhat, A. Buang, Biosorption of transition metals by freely suspended and Ca-alginate immobilised with *Chlorella vulgaris*: kinetic and equilibrium modeling, *J. Cleaner Prod.*, 171 (2018) 1361–1375.
- [56] T. Nikiforova, V. Kozlov, M. Islyaikin, Sorption of d-metal cations by keratin from aqueous solutions, *J. Environ. Chem. Eng.*, 7 (2019) 103417, doi: 10.1016/j.jece.2019.103417.
- [57] F. Dhaouadi, L. Sellaoui, M. Badawi, H.E. Reynel-Ávila, D.I. Mendoza-Castillo, J.E. Jaime-Leal, A. Bonilla-Petriciolet, A.B. Lamine, Statistical physics interpretation of the adsorption mechanism of Pb<sup>2+</sup>, Cd<sup>2+</sup> and Ni<sup>2+</sup> on chicken feathers, *J. Mol. Liq.*, 319 (2020) 114168, doi: 10.1016/j.molliq.2020.114168.
- [58] H.E. Reynel-Avila, A. Bonilla-Petriciolet, G. de la Rosa, Analysis and modeling of multicomponent sorption of heavy metals on chicken feathers using Taguchi's experimental designs and artificial neural networks, *Desal. Water Treat.*, 55 (2015) 1885–1899.